

## Immobilization of a pH-low insertion peptide onto SiO<sub>2</sub>/aminosilane-coated magnetite nanoparticles

Alexander M. Demin,<sup>\*a</sup> Timur R. Nizamov,<sup>b</sup> Alexandra G. Pershina,<sup>c,d</sup> Alexander V. Mekhaev,<sup>a</sup> Mikhail A. Uimin,<sup>e</sup> Artyom S. Minin,<sup>e</sup> Alexandra A. Zakharova,<sup>d</sup> Victor P. Krasnov,<sup>a</sup> Maxim A. Abakumov,<sup>b,f</sup> Dmitry G. Zhukov,<sup>b</sup> Alexander G. Savchenko,<sup>b</sup> Igor V. Schetinin<sup>b</sup> and Alexander G. Majouga<sup>b,f</sup>

<sup>a</sup> I. Ya. Postovsky Institute of Organic Synthesis, Ural Branch of the Russian Academy of Sciences, 620990 Ekaterinburg, Russian Federation. Fax: +7 343 369 3058; e-mail: demin@ios.uran.ru

<sup>b</sup> National University of Science and Technology 'MISIS', 119049 Moscow, Russian Federation

<sup>c</sup> Siberian State Medical University, 634050 Tomsk, Russian Federation

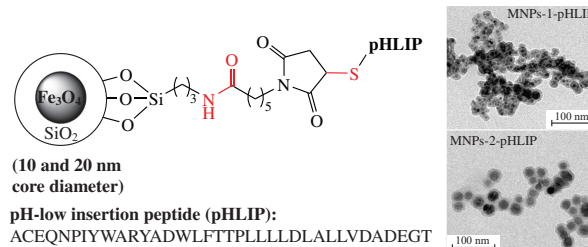
<sup>d</sup> National Research Tomsk Polytechnic University, 634050 Tomsk, Russian Federation

<sup>e</sup> M. N. Mikheev Institute of Metal Physics, Ural Branch of the Russian Academy of Sciences, 620990 Ekaterinburg, Russian Federation

<sup>f</sup> Department of Chemistry, M. V. Lomonosov Moscow State University, 119991 Moscow, Russian Federation

DOI: 10.1016/j.mencom.2019.11.008

The covalent immobilization of a pH-low insertion peptide to aminosilane-coated magnetic nanoparticles with two core diameters (10 and 20 nm) was carried out. The materials obtained were characterized by TEM, XRD, vibrating sample magnetometry, DLS, IR spectroscopy, TGA and elemental analyses. The materials did not have significant cytotoxicity, and they can be used as MRI-guided nanocarriers for tumour targeting.



Magnetic nanoparticles (MNPs) are considered as a platform for the design of contrast agents for MRI and drug delivery systems.<sup>1–4</sup> Currently, Fe<sub>3</sub>O<sub>4</sub>-based MNPs are commercially available for medical use and the development of new materials (including those for clinical applications as MRI contrasts).<sup>5</sup> The pH-low insertion peptide (pHLIP),<sup>6</sup> which inserts into the cell membrane at pH above 7.0, is successfully used as a vector molecule for targeting drugs and contrast probes to solid tumours.<sup>7,8</sup> Only a few publications considered the immobilization of pHLIP on the surface of polymeric (with a Gd<sup>III</sup> complex),<sup>9</sup> gold<sup>10,11</sup> and silica<sup>12</sup> nanoparticles for their targeting transport to the acidic tissues. Recently, we obtained pHLIP nanoconjugates of MNPs<sup>13</sup> and studied their biological activity.<sup>14</sup> Wei *et al.*<sup>15</sup> assembled MNP-pHLIP nanoclusters using poly-D-Lys and PEG derivatives. The MNP-pHLIP nanoconjugates demonstrated effective pH-responsive retention in cells and tumour tissues, and their accumulation can be controlled by MRI.<sup>14</sup>

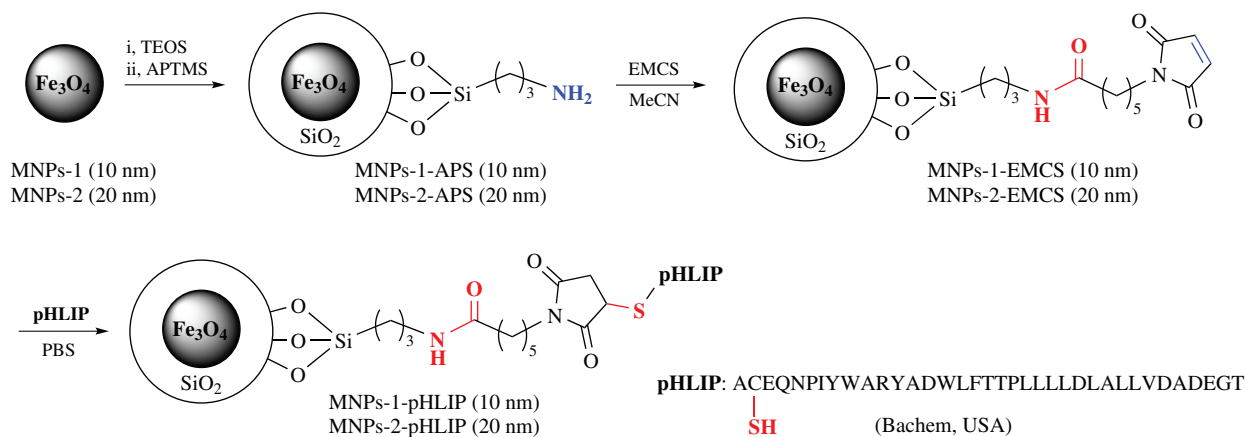
The aim of this work was to synthesize new nanoconjugates based on silica-coated MNPs and pHLIP. For this purpose, we carried out a comparative chemical modification of Fe<sub>3</sub>O<sub>4</sub> MNPs with two sorts of core size [obtained by the thermal decomposition of iron(III) oleate] by pHLIP and also a qualitative and quantitative evaluation of the peptide content on MNP surface and studied their cytotoxicity.

The thermal decomposition of iron(III) compounds has certain advantages over a precipitation method due to the possibility to obtain nanoparticles with various sizes and shapes and a narrow size distribution.<sup>16–18</sup> In this work, the thermal decomposition synthesis of nanoparticles MNPs-1 and MNPs-2 with magnetite cores 10 and 20 nm in diameter [Figures 1(a),(b)] and their coating with SiO<sub>2</sub> and 3-aminopropylsilane (APS) (Scheme 1)

were developed.<sup>†</sup> According to XRD data [Figures 1(a),(b), insert], the obtained nanoparticles had a magnetite structure (ICDD PDF-2 no. 00-019-0629); the average sizes of MNPs-1 and MNPs-2 crystallites were 7 and 14 nm, respectively, which are close to the TEM data. The sizes of MNPs-1-APS and MNPs-2-APS were 17–20 and 30–36 nm, respectively [Figures 1(c),(d)]. To preserve biological activity, pHLIP was conjugated using the thiol group of L-Cys.<sup>10</sup> For conjugation of pHLIP with nanoparticles, bifunctional cross-linkers containing the maleimide fragment are often used.<sup>12–15</sup> In this work, the immobilization of pHLIP was carried out using a 6-maleimido-hexanoic acid *N*-hydroxysuccinimide ester (EMCS) linker. On the one hand, this linker binds to amino groups on the MNPs surface by formation of an amide bond and, on the other hand, to the thiol group of the peptide by addition to a double bond of the maleimide ring (see Scheme 1).<sup>†</sup>

Note that only two examples of producing pHLIP-containing magnetic nanoconjugates were published.<sup>13–15</sup> Unlike previously synthesized nanoconjugates,<sup>13,14</sup> new nanoparticles have a protective SiO<sub>2</sub> coating. The non-covalent binding of the peptide-containing conjugate to the surface of MNPs was also carried out.<sup>15</sup> Oppositely, the peptide molecules in MNPs-1-pHLIP and MNPs-2-pHLIP were covalently bound to the MNP surface. Thus, it can be assumed that the synthesized nanoconjugates are more resistant to undesirable core oxidation and pHLIP desorption in biological media compared to MNPs.<sup>13,15</sup> In addition, the presence of a mesoporous silica coating makes it possible to load drugs on the MNPs.<sup>19</sup> Thus, the nanoparticles

<sup>†</sup> For procedures and characteristics of the nanomaterials obtained, see Online Supplementary Materials.



can be considered as promising materials for the development of targeting drug delivery systems.

According to the TEM data, after the immobilization of pHLIP, no significant changes in the morphology of the nanoparticles MNPs-1-pHLIP and MNPs-2-pHLIP were observed (16–20 and 30–36 nm, respectively) [Figures 1(e),(f)]. The specific magnetization ( $M_s$ ) of MNPs after modification decreased significantly (17 and 24 emu g<sup>-1</sup> for pHLIP-modified MNPs), probably, because of the formation of a non-magnetic silica shell on magnetic cores [Figure 1(g)]. According to the DLS data [Figure 1(h)], the average hydrodynamic diameters ( $D_h$ ) of MNPs-1-APS and MNPs-2-APS were 28 and 51 nm, and the  $\zeta$ -potentials were 38 and 40 mV, respectively. For MNPs-1-pHLIP and MNPs-2-pHLIP,  $D_h$  increased to 122 and 142 nm, respectively. The  $\zeta$ -potential of MNPs after CTAB removal from MNP surface and the immobilization of the peptide became slightly negative (−11.9 and −9.2 mV for MNPs-1-pHLIP and MNPs-2-pHLIP, respectively) and was similar to the  $\zeta$ -potential of pHLIP-containing MNPs.<sup>11–15</sup> The particle size distribution is unimodal. This can indicate the presence of individual particles and their small dynamic agglomerates in colloidal solutions.

The coating of MNPs with SiO<sub>2</sub>, APS and pHLIP was confirmed by FTIR spectroscopy data. The presence of

absorption bands at 570 cm<sup>-1</sup> ( $\nu$  Fe–O) and 1050 cm<sup>-1</sup> ( $\nu$  Si–O) in the IR spectra regions was attributed to a magnetite core and a silica shell in the nanoparticles, respectively. After MNP modification with pHLIP, in FTIR spectra a slight shift, change in the shape and intensity of the absorption bands relative to the bands of original peptide were observed: 2937 ( $\nu$  CH<sub>2</sub>), 1637 (C=O, amide I) and 1534 cm<sup>-1</sup> (N–C=O, amide II).

The amount of pHLIP on the nanoparticle surface was calculated in this work (note that there are no data on the pHLIP content of nanomaterials in refs. 9–12, 14). The peptide amount of nanoconjugates may play a crucial role in nanoparticle–cell interactions. The number of organic molecules on the MNP surface was calculated using elemental analysis data<sup>†</sup> (wt% of carbon) by analogy with previous publications.<sup>4,13,20</sup> The peptide content of pHLIP-modified MNPs was calculated by subtracting the carbon mass fraction for the EMCS-modified MNPs from the carbon mass fraction of MNPs modified with pHLIP. Thus, MNPs-1-pHLIP and MNPs-2-pHLIP contained 4.62 and 4.01  $\mu$ mol of peptide per gram of MNPs, respectively. It was close to pHLIP concentration in MNPs<sup>13</sup> (6.7  $\mu$ mol g<sup>-1</sup>). The difference in pHLIP contents can be related to the surface area of MNPs. As smaller MNPs possess a larger surface area, the peptide conjugation is more efficient.

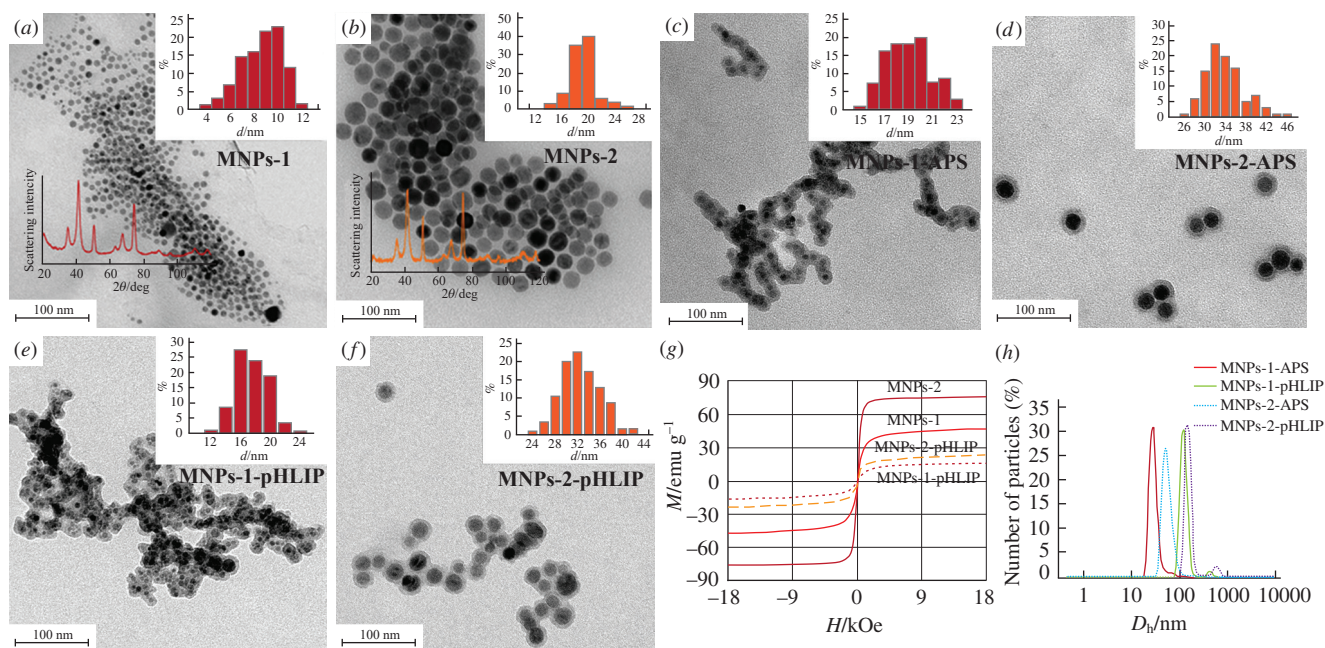


**Figure 1** (a)–(f) TEM images (on the top inserts – size distribution, on the bottom inserts in a,b – XRD patterns), (g) magnetic hysteresis loops and (h) DLS data of APS- and pHLIP-modified MNPs.

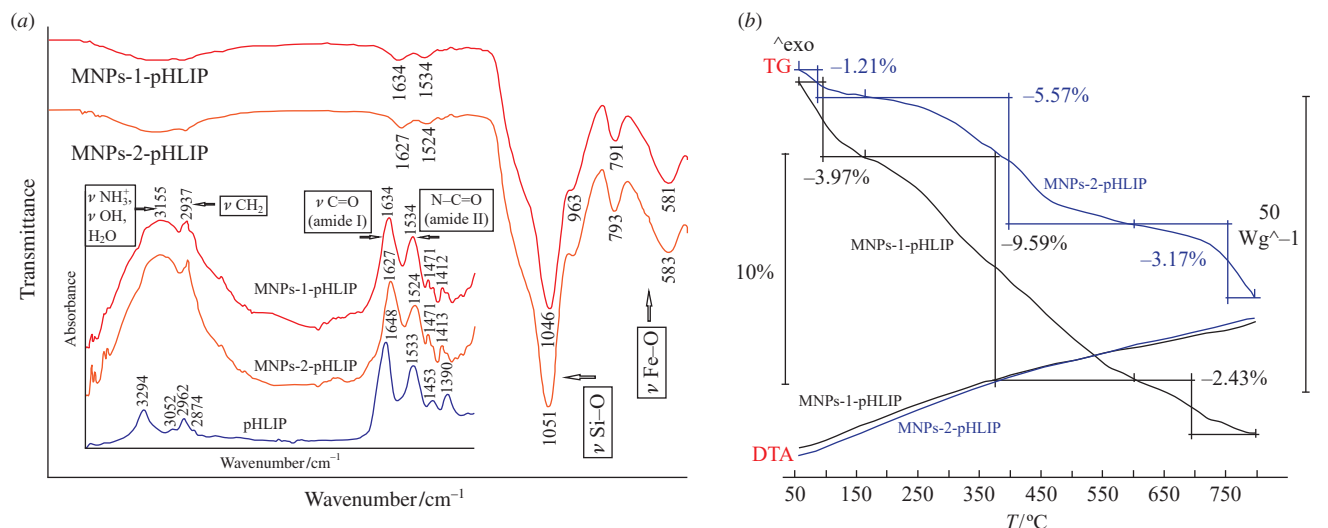


**Figure 2** (a) FTIR spectra of pHLIP and pHLIP-modified MNPs (insert: at enlarged fragment of FTIR spectra in a range of 3800–1250  $\text{cm}^{-1}$ ). (b) TGA and DTA curves of modified MNPs.

According to TGA data [Figure 2(b)], the thermal destruction of nanoconjugates includes a stage of weight loss due to the removal of physically adsorbed water (up to 160 °C) and two-stage organic coating decomposition without significant energy effects. At the second stage (160–600 °C), the thermal decomposition of organic coating takes place. The next stage of weight loss can be explained by the carbonization of organic molecules and the oxidation of a  $\text{Fe}_3\text{O}_4$  core to  $\text{Fe}_2\text{O}_3$ . Since the change in mass at the third stage can result not only from the decomposition of the organic coating, it is more rational to use only data on the weight loss at the second step of TG curves to characterize the synthesized nanoconjugates. MNPs-1-pHLIP contained at least 9.59 wt% organic coating (total quantity of APS, EMCS and pHLIP) and MNPs-2-pHLIP, 5.57 wt%. The peptide fractions in MNPs-1-pHLIP and MNPs-2-pHLIP calculated based on the elemental analysis data were up to 1.9 and 1.6 wt%, respectively.

According to the MTT assay<sup>21</sup> (Figure 3), modified MNPs at concentrations up to 100  $\text{mg dm}^{-3}$  did not show a significant cytotoxic effect on the test cells (for details, see Online Supplementary Materials).

Thus, new nanoconjugates based on two size sort  $\text{Fe}_3\text{O}_4$  MNPs and pHLIP have been synthesized. The surface modification of MNPs by the peptide proceeds slightly more efficiently for the smaller nanoparticles (4.62 and 4.01  $\mu\text{mol g}^{-1}$

for MNPs-1-pHLIP and MNPs-2-pHLIP, respectively). The resulting materials are nontoxic and possess high magnetic and MRI contrast properties. Due to the presence of mesoporous silica coatings suitable for drug loading, they can be considered as promising materials for the further development of drug delivery systems for tumour therapy.

This work was supported by the Russian Science Foundation (project no. 17-14-01316). Characterization of MNPs by IR spectroscopy, thermogravimetric and elemental analysis was performed within the framework of a state assignment theme (no. AAAA-A19-119011790130-3) using the equipment of the Centre for Joint Use ‘Spectroscopy and Analysis of Organic Compounds’ (I. Ya. Postovsky Institute of Organic Synthesis). The magnetic properties were studied within a state assignment (theme no. AAAA-A18-118020290129-5). The iron concentration measurements were carried out using the core facilities of TPU and funded from VIU-RSCBS-142/2019 and the experimental calculations were carried out at Tomsk Polytechnic University within the framework of Tomsk Polytechnic University Competitiveness Enhancement Program grant.

#### Online Supplementary Materials

Supplementary data associated with this article can be found in the online version at doi: 10.1016/j.mencom.2019.11.008.

#### References

- 1 Y. Hu, S. Mignani, J.-P. Majoral, M. Shen and X. Shi, *Chem. Soc. Rev.*, 2018, **47**, 1874.
- 2 A. Semkina, M. Abakumov, N. Grinenko, A. Abakumov, A. Skorikov, E. Mironova, G. Davydova, A. G. Majouga, N. Nukolova, A. Kabanov and V. Chekhonin, *Colloids Surf., B*, 2015, **136**, 1073.
- 3 A. M. Demin, A. G. Pershina, V. V. Ivanov, K. V. Nevskaya, O. B. Shevelev, A. S. Minin, I. V. Byzov, A. E. Sazonov, V. P. Krasnov and L. M. Ogorodova, *Int. J. Nanomed.*, 2016, **11**, 4451.
- 4 A. M. Demin, A. G. Pershina, A. S. Minin, A. V. Mekhaev, V. V. Ivanov, S. P. Lezhava, A. A. Zakharova, I. V. Byzov, M. A. Uimin, V. P. Krasnov and L. M. Ogorodova, *Langmuir*, 2018, **34**, 3449.
- 5 S. Kralj, T. Potrč, P. Kocbek, S. Marchesan and D. Makovec, *Curr. Med. Chem.*, 2017, **24**, 454.
- 6 J. C. Deacon, D. M. Engelman and F. N. Barrera, *Arch. Biochem. Biophys.*, 2015, **565**, 40.
- 7 M. C. M. Arachchige, Y. K. Reshetnyak and O. A. Andreev, *J. Biotechnol.*, 2015, **202**, 88.
- 8 L. C. Wyatt, A. Moshnikova, T. Crawford, D. M. Engelman, O. A. Andreev and Ya. K. Reshetnyak, *PNAS*, 2018, **115**, E2811.

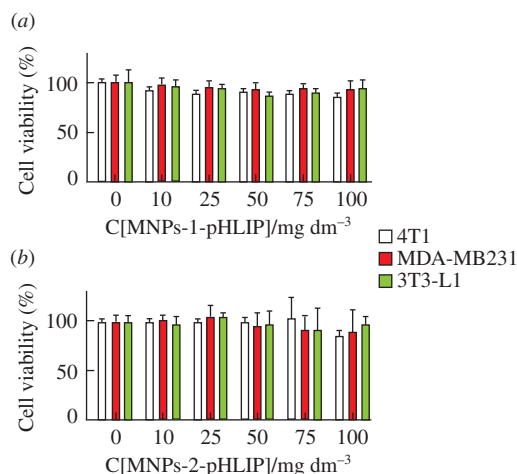


**Figure 3** MTT assay of cell viability for pHLIP-modified MNPs.

- 9 B. Janic, M. P. I. Bhuiyan, J. R. Ewing and M. M. Ali, *ACS Sens.*, 2016, **1**, 975.
- 10 L. Yao, J. Daniels, A. Moshnikova, S. Kuznetsov, A. Ahmed, D. M. Engelman, Y. K. Reshetnyak and O. A. Andreev, *Proc. Natl. Acad. Sci. U. S. A.*, 2013, **110**, 465.
- 11 Y. Tian, Y. Zhang, Z. Teng, W. Tian, S. Luo, X. Kong, X. Su, Y. Tang, S. Wang and G. Lu, *ACS Appl. Mater. Interfaces*, 2017, **9**, 2114.
- 12 Y. Zhang, M. Dang, Y. Tian, Y. Zhu, W. Liu, W. Tian, Y. Su, Q. Ni, C. Xu, N. Lu, J. Tao, Y. Li, S. Zhao, Y. Zhao, Z. Yang, L. Sun, Z. Teng and G. Lu, *ACS Appl. Mater. Interfaces*, 2017, **9**, 30543.
- 13 A. M. Demin, A. G. Pershina, K. V. Nevskaya, L. V. Efimova, N. N. Shchegoleva, M. A. Uimin, D. K. Kuznetsov, V. Ya. Shur, V. P. Krasnov and L. M. Ogorodova, *RSC Adv.*, 2016, **6**, 60196.
- 14 A. G. Pershina, O. Ya. Brikunova, A. M. Demin, O. B. Shevelev, I. A. Razumov, E. L. Zavjalov, D. Malkeyeva, E. Kiseleva, N. V. Krakhmal', S. V. Vtorushin, V. L. Yarnykh, V. V. Ivanov, R. I. Pleshko, V. P. Krasnov and L. M. Ogorodova, *Nanomedicine: NBM*, 2020, **23**, in press (<https://doi.org/10.1016/j.nano.2019.102086>).
- 15 Y. Wei, R. Liao, A. A. Mahmood, H. Xu and Q. Zhou, *Acta Biomater.*, 2017, **55**, 194.
- 16 A. A. Nikitin, I. V. Shchetinin, N. Yu. Tabachkova, M. A. Soldatov, A. V. Soldatov, N. V. Sviridenkova, E. K. Beloglazkina, A. G. Savchenko, M. A. Abakumov and A. G. Majouga, *Langmuir*, 2018, **34**, 4640.
- 17 J. Park, K. An, Y. Hwang, J.-G. Park, H.-J. Noh, J.-Y. Kim, J.-H. Park, N.-M. Hwang and T. Hyeon, *Nat. Mater.*, 2004, **3**, 891.
- 18 J. Kim, H. S. Kim, N. Lee, T. Kim, H. Kim, T. Yu, I. C. Song, W. K. Moon and T. Hyeon, *Angew. Chem., Int. Ed.*, 2008, **47**, 8438.
- 19 M. Colilla, B. González and M. Vallet-Regí, *Biomater. Sci.*, 2013, **1**, 114.
- 20 A. M. Demin, A. Yu. Vigorov, I. A. Nizova, M. A. Uimin, N. N. Shchegoleva, A. E. Ermakov, V. P. Krasnov and V. N. Charushin, *Mendeleev Commun.*, 2014, **24**, 20.
- 21 T. Mosmann, *J. Immunol. Methods*, 1983, **65**, 55.

Received: 1st April 2019; Com. 19/5868